The habenula clock regulates response to a stressor

Adriana Basnakova[1, 2], Ruey-Kuang Cheng[3], Joanne Chia Shu Ming[3] and Suresh Jesuthasan[2, 3]

[1]School of Biological Sciences, University of Manchester, UK.

[2]Institute of Molecular and Cell Biology, Singapore.

[3]Lee Kong Chian School of Medicine, Nanyang Technological University, Singapore.

Abstract

The lateral habenula, a regulator of neuromodulators that is activated by aversive stimuli, contains a molecular clock whose significance is unknown. Here, using zebrafish, we test the hypothesis that the habenula clock affects the switch in internal state that is triggered by an aversive stimulus. Consistent with the expression of clock genes, habenula neural activity varies in a circadian manner. Disruption of clock function, by expression of a truncated clock gene specifically in the habenula, did not affect acute responses to the alarm pheromone *Schreckstoff*. However, behaviours elicited by transient exposure to *Schreckstoff*, namely freezing in a novel environment and dark avoidance, were reduced. Behaviours that are regulated by the pineal clock and not triggered by stressors were unaffected. These findings establish that the habenula clock independently influences the stress response induced by an aversive stimulus, indicating that this clock underlies circadian variation in response to a stressor.

Introduction

Sensory stimuli evoke a variety of responses in an animal. A stimulus with high salience, for example, will elicit changes in movement and in internal state. These changes in state, which can include increase in arousal and vigilance, outlast the presence of the stimulus and are mediated by the release of neuromodulators such as serotonin (Chaouloff et al., 1999) and dopamine (Abercrombie et al., 1989; Holly and Miczek, 2016). One regulator of

these neuromodulators in vertebrates, especially in response to aversive stimuli, is the habenula (Namboodiri et al., 2016). The habenula, which is located in the epithalamus, consists of two domains, medial and lateral, with the latter controlling dopamine and serotonin release from the ventral tegmental area (VTA) and raphe, respectively. Exposure to a stressor increases the level of activity in lateral habenula neurons (Andalman et al., 2019), and abnormal firing in the lateral habenula is associated with maladaptive behaviours (Li et al., 2013; Yang et al., 2018). Thus, a knowledge of factors that influence activity in the lateral habenula is important in understanding what shapes the extended response to stressors.

One such a factor appears to be an intrinsic molecular clock. Components of the clock machinery (Takahashi, 2017), such as *per2* in mouse (Guilding et al., 2010) and rat (Zhao et al., 2015), *per1* and *bmal*1 in zebrafish (Weger et al., 2013), and *per1b* in goldfish (Sánchez-Bretaño et al., 2015), are expressed in a circadian manner in the lateral habenula. Although the habenula receives input from the master pacemaker in the suprachiasmatic nucleus (SCN) (Buijs, 1978; Sakhi et al., 2014), the habenula clock persists even when the SCN is lesioned (Salaberry et al., 2019). In general, the molecular clock drives daily variations in excitability, enabling neurons to generate rhythmic electrical output (Belle, 2015; Cao and Nitabach, 2008; Pennartz et al., 2002). In agreement with this, spontaneous firing in the habenula of rat (Zhao and Rusak, 2005) and mouse (Guilding et al., 2010; Sakhi et al., 2014) varies across a circadian cycle. It has been shown that the effect of a stressor on lateral habenula electrical activity is largest during the active period, when spontaneous activity is lowest (Chastrette et al., 1991). An implication of this is that the habenula clock influences the response to stimuli that are processed by the habenula. There is, however, no experimental evidence for this.

We hypothesize that the habenula clock acts in an autonomous manner to influence response to an aversive stimulus. It is known that the response to stressors varies with time of day (Koch et al., 2017), as can be seen with the response to a conspecific alarm substance (Di Rocco et al., 2014; Hume and Wagner, 2018), but the underlying mechanism is unclear. One strategy that can be used to investigate the function of the molecular clock

in a specific cell is to express a truncated CLOCK protein (ΔCLK) (Dekens and Whitmore, 2008). The molecular clock consists of a transcriptional-translational feedback loop (Takahashi, 2017). A heterodimer of CLOCK and BMAL enters the nucleus, where it drives transcription of *period* (*per*) and *cryptochrome* (*cry*) genes, which then inhibit the heterodimer. The truncated CLOCK protein binds BMAL, but the resulting heterodimer is unable to activate transcription of target genes. This strategy has been successfully used in the pineal of zebrafish, where expression of truncated CLOCK prevented circadian variation in clock-controlled genes in the pineal and led to a disruption of circadian rhythmicity in locomotion, sleep and vertical position (Ben-Moshe Livne et al., 2016). Here, we use the GAL4/UAS system to drive expression of ΔCLK specifically in the habenula of zebrafish. Our results demonstrate that the intrinsic habenula clock has an essential role in regulating the extended behavioural response to an aversive stimulus.

Results

The zebrafish habenula displays circadian variation in activity

The expression of clock genes in the mouse habenula is correlated with circadian changes in neural activity (Guilding et al., 2010; Sakhi et al., 2014). To assess whether there is a circadian change in neural activity in the zebrafish habenula, we used immunohistochemical detection of phosphorylated extracellular signal-regulated kinase (pERK), which has the advantage of reporting neural activity in freely swimming animals (Randlett et al., 2015), and has been used to examine circadian activity in the mouse SCN (Hughes et al., 2004). In 8 day old zebrafish, pERK label was evident in both nuclei and the cytoplasm of scattered neurons, since pERK translocates to the nucleus upon neuronal activation (Plotnikov et al., 2011). Generally, pERK label was more prominent in the lateral (or ventral) habenula compared to the medial (or dorsal) habenula (compare cells indicated with white arrowheads in Figure 1A and B). Label was also seen in neuropils (Figure 1A), where pERK potentially regulates synaptic plasticity by influencing the trafficking and distribution of local substrates (Mao and Wang, 2016). To determine if there is any consistent difference in activity between day and night, registered and scaled image

data was first normalized by calculating the pERK/total-ERK (tERK) ratio. The normalized image data was then compared between 'Day' and 'Night' groups, which consisted of > 100 zebrafish larvae fixed at Zeitgeber time ZT3 (3 hours after lights on; Figure 1D, G) and ZT15 (Figure 1C, F) respectively. A pixel-wise 'Night'-over-'Day' comparison, implementing a false discovery rate threshold of 0.1%, (Figure 1E, H) indicates that levels of pERK were higher at night relative to the day, especially in the lateral habenula. The day-night difference was also seen in the lateral habenula of fish held in constant darkness (Figure 2), although to a lesser extent than fish that had undergone a normal light-dark cycle. This suggests that, while light has a role, neural activity in the lateral habenula is influenced by a circadian clock.

Disruption of the habenula clock reduces the post-exposure effects of *Schreckstoff*

To selectively express ΔCLK in the habenula, we used the GAL4/UAS system with *TgBAC(gng8:GAL4)* (Hong et al., 2013) as the driver. In addition to ΔCLK, the effector construct also included enhanced green fluorescent protein (EGFP), which was separated from ΔCLK by a 2A peptide linker, thus enabling the expression of two separate proteins. The presence of EGFP in the habenula neurons of *Tg(gng8:GAL4, UAS:EGFP-ΔCLK)* fish (Figure 3A, B) indicates that the construct is expressed appropriately and enables convenient identification of ΔCLK+ individuals (Ben-Moshe Livne et al., 2016). Labelling with an antibody against the Myc tag, which is fused in frame at the C-terminus of ΔCLK, indicates that the truncated CLOCK protein is translated (Fig. 3C). To assess whether ΔCLK expression had an effect on physiological function of the habenula, brains were isolated from adult zebrafish expressing EGFP-ΔCLK, and from their non-expressing siblings, at two different time points, ZT3 and ZT15. The supernatant from extracts were analyzed by liquid chromatography and mass spectrometry (LC/MS) (Chatterjee and Gerlai, 2009). While non-expressing fish had a clear difference in the day- and night-time levels of dopamine (DA), there was almost no difference in fish expressing ΔCLK protein (Figure 4). The difference in day-night serotonin (5-HT) levels was also reduced in the ΔCLK+ fish,

although to a lesser extent. These results indicate that expression of ΔCLK in the habenula is effective in disrupting the intrinsic molecular clock.

We asked whether behavioural responses to an aversive stimulus are affected by the expression of ΔCLK. One aversive stimulus for fish is the alarm pheromone *Schreckstoff* (Pfeiffer, 1962). This substance elicits activity in the lateral habenula (Jesuthasan et al., 2020), and the behavioural response is modified by disruptions of this structure (Ogawa et al., 2014). Importantly, the effects of *Schreckstoff* vary with time of day (Thines and Vandenbussche, 1966). In adult zebrafish, *Schreckstoff* causes an acute change in swimming speed and tank position (Jesuthasan and Mathuru, 2008; Speedie and Gerlai, 2008). Even after being removed from water containing *Schreckstoff*, adult fish display persistent stress, as indicated by abnormal scototaxis and elevated levels of serotonin (Maximino et al., 2014), as well as increased alertness (Pfeiffer and Riegelbauer, 1978). Similarly, it was recently shown that larval zebrafish display persistent stress following transient exposure to the alarm substance, as indicated by increased dark avoidance (Jesuthasan et al., 2020). These persistent behavioural effects are accompanied by a sustained change in brain state, as shown by calcium imaging (Jesuthasan et al., 2020).

To monitor the acute response, adult fish were placed individually in a test tank. After a period of acclimatization, the alarm substance was introduced into the tank. Adult *Tg(gng8:GAL4, UAS:EGFP-ΔCLK)* zebrafish, like their non-expressing siblings, showed an increase in darting and moved to the base of the tank, with a number of fish then freezing (Figure 5A-E). To monitor post-exposure behaviour, individual fish were exposed to the alarm substance in a beaker, then transferred to a novel tank. ΔCLK fish, in contrast to their non-expressing siblings, did not freeze, but behaved similarly to fish that had been exposed to fish water (Figure 5F, G). We also monitored the post-exposure behaviour of larval zebrafish, using a light-dark choice assay (Steenbergen et al., 2011). In comparison to their non-expressing siblings, larval *Tg(gng8:GAL4, UAS:EGFP-ΔCLK*) fish displayed less dark avoidance after transient exposure to *Schreckstoff*, as indicated by the amount of time spent in the dark side of the tank (Figure 5H, I). Together, these observations indicate that

disruption of the habenula clock leaves acute responses unaffected but reduces the persistent stress response that is evoked by transient exposure to the alarm substance.

Expression of ΔCLK in the habenula does not affect pineal-regulated circadian behaviour

As a measure of the specificity of expressing ΔCLK in the habenula, we examined circadian behaviours that are under the control of the pineal clock (Ben-Moshe Livne et al., 2016). We first analyzed the rhythmic locomotor activity (Prober et al., 2006) of ΔCLK+ larvae and their control (CTRL) siblings. All larvae were entrained to the standard light-dark (LD) cycle and their locomotion was monitored for a few hours during the light phase, followed by the onset of darkness at ZT14 for activity tracking during the night. Subsequently, the fish were monitored for one day under constant darkness (DD), in order to eliminate the masking effects of light and dark on clock-regulated behavior (Ben-Moshe Livne et al., 2016). As seen in Figure 6, ΔCLK+ larvae showed a similar pattern of locomotion as their non-expressing siblings, becoming mobile during the light phase and during the subjective day, while exhibiting quiescent periods of inactivity during the 1st and 2nd night of the recording.

In addition to locomotion, we also examined arousal threshold, which is normally elevated during the sleep-like state at night. Arousal threshold was measured by responsiveness to auditory stimuli (Zhdanova et al., 2001). Nine different intensities were delivered between ZT17 and ZT23, and a sudden change in locomotion was taken as an indicator of responsiveness (Figure 6F, G). A larva was scored as a responder if it moved more than 7 pixels after the stimulus and the average percentage of responders was calculated for each stimulus intensity per group for each experimental run (N = 5 experimental runs). Overall, no difference was seen between ΔCLK+ larvae and their control siblings (Figure 6I). Together, these experiments indicate that disruption of the habenula clock has relatively specific effects.

Discussion

All aspects of life, from arousal state (Scammell et al., 2017) to the ability to handle stress (Daut and Fonken, 2019) and respond to rewards (Antle and Silver, 2016; McClung et al., 2005), vary with time of day. This reflects the tight control exerted by the circadian clock on the physiology and behavior of animals. Clock genes, which drive the circadian clock, are expressed broadly in the brain (Moore and Whitmore, 2014; Shearman et al., 1997; Shieh, 2003; Sun et al., 1997). In this paper, we investigated the hypothesis that the habenula clock influences the stress response triggered by an aversive stimulus. Such stimuli are known to trigger the release of neuromodulators, which cause an extended change in internal state and thus in behaviour (Anderson and Adolphs, 2014), and the habenula is a part of the circuit mediating stimulus-mediated neuromodulator release. To test this hypothesis, we expressed a dominant negative mutant of the *clock* gene (Dekens and Whitmore, 2008) specifically in the zebrafish habenula. Expression of ΔCLK protein in the habenula reduced freezing and dark avoidance induced by the alarm substance. The darting and downward movement to the alarm substance itself was not affected, consistent with the hypothesis that the habenula primarily affects the change of internal state that follows exposure to the alarm substance. Although we detected a change in circadian variation of dopamine and serotonin, no change in circadian behaviours, such as locomotion or arousal, was observed. This may reflect the fact that habenula-controlled neuromodulators are not critical in these behaviours, which are not evoked by stressors. Together, these observations indicate that the behavioural consequence of disruption of the habenula clock is restricted primarily to stress responses. This contrasts with the broader phenotype seen with pineal-specific disruption of the clock (Ben-Moshe Livne et al., 2016).

One possible mechanism for the reduced stress response in fish expressing ΔCLK is that the net change in stimulus-evoked activity is lower. As shown in this paper, activity in the zebrafish lateral habenula is higher at night. Expression of ΔCLK blocks transcription of *per* (Dekens and Whitmore, 2008), which is predicted to place habenula neurons in the 'night state' throughout the circadian cycle. Consistent with this, the day-time levels of dopamine

and serotonin in ΔCLK fish were similar to night-time levels. A higher level of activity means that an incoming stimulus will cause a relatively small change in output. In contrast, the same stimulus will have a stronger effect in a fish with low spontaneous activity in the habenula. This interpretation is in line with the finding of Chastrette and colleagues (Chastrette et al., 1991) that the effect of a stressor on the habenula of rats is higher during the active period, when spontaneous activity is low. The observation that the alarm response in diurnal fish is reduced at night (Thines and Vandenbussche, 1966) is consistent with this.

Mechanisms that control spontaneous activity in the lateral habenula are one area of growing interest in mental health, given that increased activity here is linked to abnormal stress responses (Andalman et al., 2019; Li et al., 2013; Yang et al., 2018). The findings here suggest that a potential way forward is to manipulate the clock specifically in the habenula, given the relatively specific effects seen. It may also be useful to screen for clock-regulated genes. This could be done by single-cell RNAseq of habenula neurons at different times of the day, for example, and may lead to the identification of ion channels or other molecules that regulate intrinsic activity and excitability of habenula neurons. This knowledge may lead to an improvement in the treatment of stress disorders such as anxiety.

Materials and Methods

Transgenic lines

TgBAC(gng8:GAL4)^{c426} (Hong et al., 2013) was used to drive expression in the habenula. Tg(UAS:EGFP-ΔCLK) was generated by injection of pT2-UAS:EGFP-2A-ΔCLK-5xMYC using Tol2 mediated transgenesis. All experiments were carried out under guidelines approved by the IACUC of Biopolis (181408) and NTU (A19014).

224 ## pERK analysis

225 ### *Immunohistochemistry*

226 Fish of *nacre* background were randomly split into 'Day' and 'Night' groups. Fish were
227 raised at a density of ~0.125 fish/mL and maintained at 28°C under 14-10 h LD cycle,
228 henceforth referred to as standard conditions. For the comparison under DD, tanks with
229 the larvae were transferred into a dark box at ZT14 the day before fixation.
230
231 Larvae at the age of 8 dpf were fixed at Zeitgeber time ZT3 and ZT15 or circadian time
232 (CT)3 and CT15, based on findings that the peak and trough of *per3* expression occurs at
233 ZT3 and ZT15, respectively (Moore and Whitmore, 2014). Immediate and consistent
234 fixation was achieved by pouring the water containing the larvae through a fine sieve that
235 was immediately placed in ice-cold 4% paraformaldehyde (PFA) in phosphate buffered
236 saline (PBS). Fixations at ZT15, CT3 and CT15 were performed under dim light. Incubation
237 in the fixative was carried out at 4ºC for ~22h. Fixed larvae were then stored in 100%
238 methanol at -20˚C for several days. Larvae were rehydrated by successive 5-minute washes
239 in 70%, 50%, 25% and 0% methanol in PBS, then placed in PBST [1 % Bovine serum
240 albumin (Sigma) + 1 % dimethyl sulfoxide (DMSO) + 0.1% Triton-X 100 in PBS] for 1 h at
241 room temperature. They were then incubated in primary antibodies ((rabbit anti-pERK
242 (Cell Signalling, #4370) and mouse anti-tERK (Cell Signalling, #4696), both diluted at
243 1:500) at 4°C for 3-4 days. Samples were washed five times in PBST and then incubated in
244 secondary antibodies (Alexa Fluor 647 goat anti-rabbit (ThermoFisher) and Alexa Fluor
245 488 goat anti-mouse (ThermoFisher), both diluted at 1:500) for 2 h at room temperature.
246 Samples in which the primary antibody was omitted were run in parallel to test the
247 specificity of the secondary antibody binding.

248 ### *Confocal imaging*

249 Larvae were mounted in 2% low melting agarose (LMA) in PBS and imaged using a Zeiss
250 LSM800 upright confocal microscope equipped with 40X 1.0 NA water dipping objective.
251 The acquisition settings were kept consistent in all experiments. Images were collected at
252 512x512 resolution. The habenula was imaged with parts of the forebrain (pallium and

253 subpallium) to improve image registration. The number of frames was set to cover the
254 whole depth of habenula and varied across samples, which was later corrected during the
255 registration.

256 ***Image registration and data analysis***

257 In order to efficiently compare pERK signals between 'Day' and 'Night' groups, all confocal
258 stacks were first aligned so that each voxel covered an approximately equivalent physical
259 location in each sample. This was achieved by non-rigid registration of the images to a
260 single reference image using the homogenous anti-tERK staining. The registration was
261 carried out with the Computational Morphometry Toolkit (CMTK,
262 http://www.nitrc.org/projects/cmtk/) and the command string (-awr 010203 -T 4 -X 52 -C
263 8 -G 80 -R 3 -A '--accuracy 0.4' -W '--accuracy 1.6'). Registered stacks were scaled down to
264 150/150/30 (x/y/z) resolution and the image noise was reduced with 2D Gaussian filter
265 (sigma = 2) using the 'PrepareStacksForMAPMapping.ijm' macro in FIJI software
266 (http://engertlab.fas.harvard.edu/Z-Brain/ (Randlett et al., 2015)). Image data was then
267 normalized by calculating pERK/tERK ratio and a pairwise comparison between 'Day' and
268 'Night' groups was carried out at each pixel as follows: first pseudo groups were randomly
269 generated containing equal number of fish from both groups and Mann-Whitney U
270 statistics Z-score was calculated over 500 iterations, producing a distribution of Z-scores.
271 Assuming the normal distribution, a Z-score value corresponding to the false discovery rate
272 of 0.1% was then used as a threshold so that if the Z-score value of the 'Day' vs 'Night'
273 comparison was higher than the threshold it was considered significant. Application of the
274 false discovery rate of 0.1% as a threshold was justified by a control comparison of
275 randomly created mixed groups. The pixels which were significantly different during the
276 final 'Night'-over-'Day' comparison, during which 'Day' group served as a baseline, were
277 then assigned a colour where green and magenta represented significant increase and
278 decrease, respectively, in the 'Night' group. Those pixels were also allocated intensity
279 values within the range of 0:65535 according to the size of delta between the median
280 values of the two groups (i.e. the lowest and highest intensities indicated the smallest and
281 largest deltas within the range of 0:0.5, correspondingly). The pixels which did not exhibit
282 significant difference were not assigned any colour. All data were analysed using the

283 'MakeTheMAPMap.m' script (http://engertlab.fas.harvard.edu/Z-Brain/, (Randlett et al.,
284 2015)) in Matlab (Mathworks).

285 Immunohistochemistry and imaging of EGFP-ΔCLK

286 The *Tg(gng8:GAL4,UAS:EGFP-ΔCLK)* larvae at the age of 7 dpf were fixed in 4% PFA at 4ºC
287 for ~22 h. For immunostaining of extracted brains, skin covering the brain was manually
288 removed and exposed brains were washed 3 times in PBST. Antigen retrieval was
289 performed by incubating the fish in 150 mM Tris-HCl (pH 9.0) for 5 min at room
290 temperature in order to equilibrate, and by subsequent heating of the samples at 70˚C for
291 15 min. Following several washes and a blocking step, samples were incubated in the
292 rabbit anti-GFP primary antibody (Torrey Pines Biolabs Inc., #TP401), diluted 1:500, and
293 the mouse anti-Myc antibody (9E10; Santa Cruz Biotechnology), diluted 1:100, at 4ºC for a
294 few days. The secondary antibodies used were Alexa Fluor 488 goat anti-rabbit
295 (ThermoFisher and Abcam), diluted 1:1000, and Alexa Fluor 647 goat anti-mouse
296 (ThermoFisher), diluted 1:500. The immunostained brains were mounted in 2% LMA in
297 PBS and imaged using a Zeiss LSM800 confocal microscope equipped with 40X water
298 immersion objective.

299 Screening and selection of *Tg(gng8:GAL4,UAS:EGFP-ΔCLK)* fish

300 All of the *Tg(gng8:GAL4,UAS:EGFP-ΔCLK)* fish used in the following experiments were first
301 screened for GFP fluorescence at 3 dpf using a Olympus MVX10 stereo fluorescence
302 microscope. Since the expression of EGFP-ΔCLK in the habenula was mosaic, only
303 individuals with expression in the majority of habenula cells were selected and used for
304 further experiments as ΔCLK-positive (ΔCLK+) fish. Individuals with zero expression as
305 well as larvae exhibiting a minimal number of randomly labelled cells (less than ~15 cells
306 per habenula) were used as the control (CTRL) siblings (Figure S1). Following the
307 behavioural experiments, larvae were immobilized in tricaine methanesulfonate (MS-222;
308 final concentration of 0.01 mg/ml; Sigma), mounted in 2% LMA in E3 medium and the
309 habenula-specific expression of EGFP was assessed using a Zeiss LSM800 confocal
310 microscope and 40X water dipping objective.

Quantification of DA and 5-HT levels

Three-month old female ΔCLK+ fish and their CTRL siblings were immobilized using iced water and euthanized by decapitation at ZT3 and ZT15. Whole brains, excluding the olfactory bulb, were extracted in the ice-cold Ringer's solution (116 mM NaCl, 2.9 mM KCl, 1.8 mM $CaCl_2$, 5.0 mM HEPES, pH 7.2), snap-frozen in liquid nitrogen and stored in -80˚C until further analysis. Supernatant was collected as described in (Chatterjee and Gerlai, 2009). Quantification of dopamine (DA) and serotonin (5-HT) was carried out by LC/MS using the following analytical standards: dopamine hydrochloride (D2960000: Sigma-Aldrich), dopamine-1,1,2,2-$d_4$hydrochloride (73483: Sigma-Aldrich) and serotonin (14927: Sigma-Aldrich). Data were analyzed and plotted using Estimation Statistics (Ho et al., 2019).

Behaviour assays

Locomotor activity

The *Tg(gng8:GAL4,UAS:EGFP-ΔCLK)* larvae were raised under standard conditions. Each experimental run involved animals from the same batch, originating from one pair of parents. The larvae were screened and selected as described in the previous section. At the age of 6 dpf the larvae were placed individually in a 24-well plate filled with 1.5 ml of tank water per well. The plate was then transferred into an incubator equipped with an IR camera (acA2040-90µm USB 3.0: Basler), a white LED box and four IR LED bars (LBS2-00-080-3-IR850-24V, 850 nm: TMS Lite). The camera and the LEDs were connected to a PC via a microcontroller board (Arduino UNO SMD). At the onset of recording (ZT6 – 9), fish were kept under ambient light, which was switched off at ZT14 (10 PM) and was kept off during the next day for the monitoring of activity under DD. A customized script written in Python 2.7, incorporating functions from the OpenCV library was used to control the Arduino microcontroller and simultaneously video-track fish locomotor activity. The video was captured using 576 x 864-pixel resolution at 10 frames per second and the background subtraction method was implemented to extract the 'x' and 'y' coordinates of each fish online. The position data was then converted to total distance (mm) travelled by each fish

339 per 1 min time. The data conversion, further analysis and plotting were carried out using
340 custom-written Excel macros, Python 2.7 and Estimation Statistics (Ho et al., 2019).

341 ***Arousal threshold***

342 Six days-old ΔCLK+ larvae and their CTRL siblings were randomly placed in a 24-well plate
343 and their locomotor activity was video-tracked as described in the previous section. In
344 order to assess the arousal during sleep, vibration stimuli were applied through a speaker
345 controlled, via an Arduino microcontroller board, by a modified version of the activity-
346 tracking code in Python 2.7. Starting at ZT17, eighteen stimuli of nine different intensities,
347 where 50% of computer audio output represented the highest intensity, were delivered for
348 200 ms (starting from 0%) in 12-16% increments every minute, first in a descending and
349 then ascending order. The time interval between stimuli was determined based on
350 previous findings that suggest a 30-second inter-stimulus gap is sufficient to avoid
351 behavioral habituation (Burgess and Granato, 2007). The protocol was repeated at the
352 commencement of every hour until ZT22, while the onset by ascending or descending
353 order was altered each time. In total, 12 replicates of each stimulus intensity were
354 generated. A fish was scored as responding if it moved more than 7 pixels (~ 4 mm)
355 following the stimulus delivery and the average percentage of responding fish was
356 calculated for each of the stimulus intensities (Woods et al., 2014). The observed values
357 were corrected for variations in the baseline locomotor activity, by first calculating the
358 background probability of locomotion as a percentage of larvae which moved more than 7
359 pixels 5 s before the application of each stimulus. The average of 108 measures of the
360 background probability of locomotion was then used to calculate the corrected probability
361 of response at each of the stimulus intensities, implementing the following equation:
362 corrected probability of response = observed value x [(observed value - background offset)
363 / (max observed value - background offset)] (Woods et al., 2014).

364 ***Novel tank assay***

365 All experiments were conducted between ZT2 and ZT4 on 3-5 month-old adult zebrafish,
366 closely following the protocol of (Haghani et al., 2019)). Fish were recorded in pairs in a
367 darkened room with a black background, where tanks were illuminated from the top with a
368 natural light LED bar. Novel tanks were made of glass measuring 20 cm (L) by 5 cm (W) by

369 12 cm (H) with opaque sides (to prevent fish from viewing each other), placed side by side.
370 Fresh water from the facility was added to tanks up to the 10 mL mark to make a total
371 volume of 1 L. The setup was placed within a curtained area to obscure the experimenter.
372
373 Prior to exposure to the novel tank, fish were handled carefully to ensure that handling
374 stress was minimised. Fish were gently netted in pairs from their home tanks in the facility
375 to smaller crossing tanks, where they were brought into the room with the behavioural
376 setup. Then, fish were netted into 100 mL beakers with ~30 mL of fish facility water and
377 quickly poured into the novel tank. The recording was started within 30 s of fish being in
378 the recording tanks. For exposure to *Schreckstoff,* fish were placed in 100 mL beakers
379 containing 200 µL of heated skin extract (see (Chia et al., 2019) for extraction method) in
380 50 mL fish facility water for 2 minutes. Fish were netted into another beaker containing
381 fresh facility water before being poured into the novel tank. Videos were acquired at 10
382 frames per second for 600 s (10 mins) using a Basler Ace camera (acA1300–200 µm; 1,280
383 × 1,024). The position (x-y coordinates) of the fish were tracked, and speed was binned by
384 mm/s into a probability density curve.
385
386 For acute exposure to *Schreckstoff*, fish were first habituated in the glass tanks for 5-7 mins.
387 Then, fish were recorded in the tanks for 5 mins before 1 mL of 1:4 dilution of heated skin
388 extract was pipetted into the tanks. The recording continued for 5 mins after *Schreckstoff*
389 delivery for the alarm response to be observed. Characteristic alarm behaviours were
390 quantified, such as time spent in the bottom third of the tank, number of darting episodes
391 (fish speed >5 SD above average swim speed for the first 5 mins), and number of freezing
392 episodes (movement of <5.5 mm per second).

393 ***Light/dark choice assay***

394 All experiments were performed between ZT2 and ZT9 in a behavioral arena within
395 blackout curtains as described previously (Cheng et al., 2016). Four transparent plastic
396 tanks (dimensions: 43 mm W × 60 mm L × 30 mm H) filled with 30 mL fresh tank water
397 served as assay chambers. Opaque cardboard sheets were placed between the 4 tanks.
398 Tanks were placed on an Apple iPad screen and videos (9 fps) were recorded on a USB3.0

Basler camera (Model# acA2040-90umNIR 1440 × 1080 pixels) with a long-pass filter (MIDOPT, LP830 830nm) placed above. Two IR light bars (850 nm peak from TMS-lite) positioned next to the 4 tanks served as an IR light source. The light/dark compartments were created by white and black rectangles (with 50% transparency level for the black) on a Microsoft PowerPoint slide displayed on the iPad Air at highest brightness level.

Larvae were exposed either to *Schreckstoff* or to control water (embryo medium) in a treatment tank of the same dimensions with the same volume of tank water for 10 minutes. Larvae were then gently pipetted from the treatment tank into two wash-out tanks sequentially before being placed into the dark/light test chamber. Real-time tracking of the fish was achieved by custom-written Python codes using the OpenCV library and recorded as coordinates of the centroid of the fish across time. Larval behavior was recorded for 10 minutes. Offline analysis was performed using custom-written Excel macros to determine the position of the animals, the number of entries into each compartment, the percentage of total time spent in each compartment, etc. A few fish (n=2 in both the Control group and Gng8/ΔCLK group) were excluded from the analysis because they were entirely immobile or because of tracking errors.

Acknowledgements

This work was funded by the Singapore Ministry of Education under its Academic Research Fund Tier 2 Award (MOE2017-T2-058) and by the Lee Kong Chian School of Medicine, Nanyang Technological University Singapore, through a Start-Up Grant to SJ, and by A*Star through an ARAP fellowship to AB. We thank Yoav Gothilf for providing the pT2-UAS:EGFP-2A-ΔCLK-5xMYC construct and Marnie Halpern for providing the *TgBAC(gng8:GAL4)*^{c426} line. We also thank Hugh Piggins, David Lyons, Caroline Wee and Ajay Mathuru for comments and discussion.

Author contributions

AB, RKC and JCSM performed experiments and analyzed data. SJ and AB designed the study and wrote the manuscript.

Figures

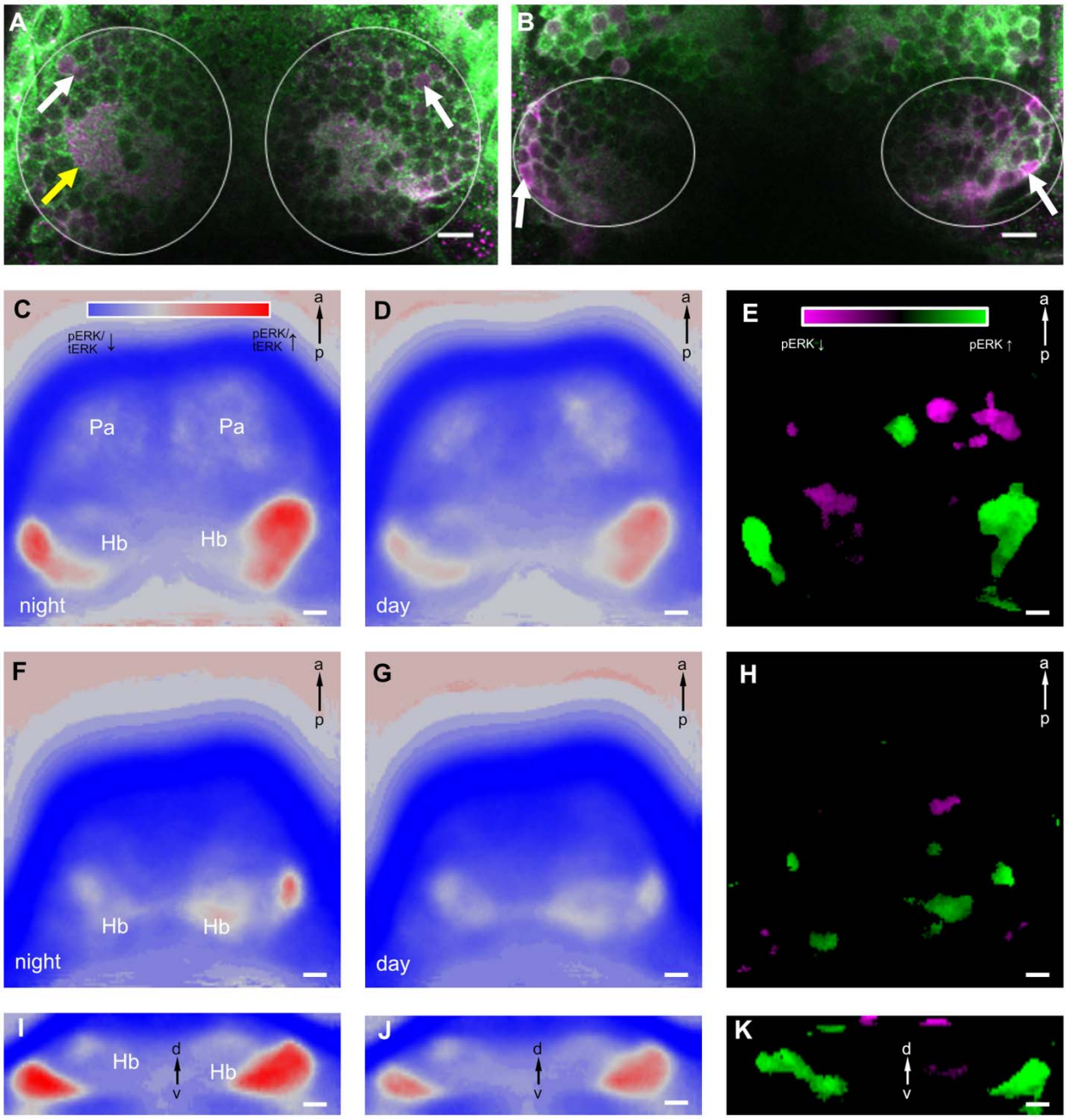

Figure 1. Day-night difference ERK phosphorylation in the habenula. (**A, B**) Immunohistochemical detection of phosphorylated ERK (pERK; magenta) and total ERK (tERK, green) at two different focal planes of the habenula, dorsal (A) and ventral (B), of an 8-day old zebrafish. The white arrows indicate labelled cell bodies, while the yellow arrow indicates the neuropil. (**C-H**) Day-Night comparison of normalized pERK levels in the

habenula. Raw images were registered, downsampled and smoothed and pERK/tERK ratio was calculated at each pixel. Median pERK/tERK levels in the habenula were calculated based on N = 102 larvae fixed during the night (C, F) and N = 130 larvae fixed during the day (D, G). Two different planes, ventral (C, D) and dorsal (F, G) are shown here. The difference in the ventral (E) and dorsal (H) planes, based on 'Night-over-Day' comparison, with green indicating higher levels of pERK at night, while magenta indicates lower levels (see wedge in panel E). (**I-K**) Reconstructed transverse section through the habenula of the stacks of median activity during the night (I), day (J) and difference (K). Strong activity is detected in the lateral region only. All images except I-K are dorsal view. Scale bar = 10 μm. a: anterior; p: posterior; d: dorsal; v: ventral; Pa: pallium; Hb: habenula.

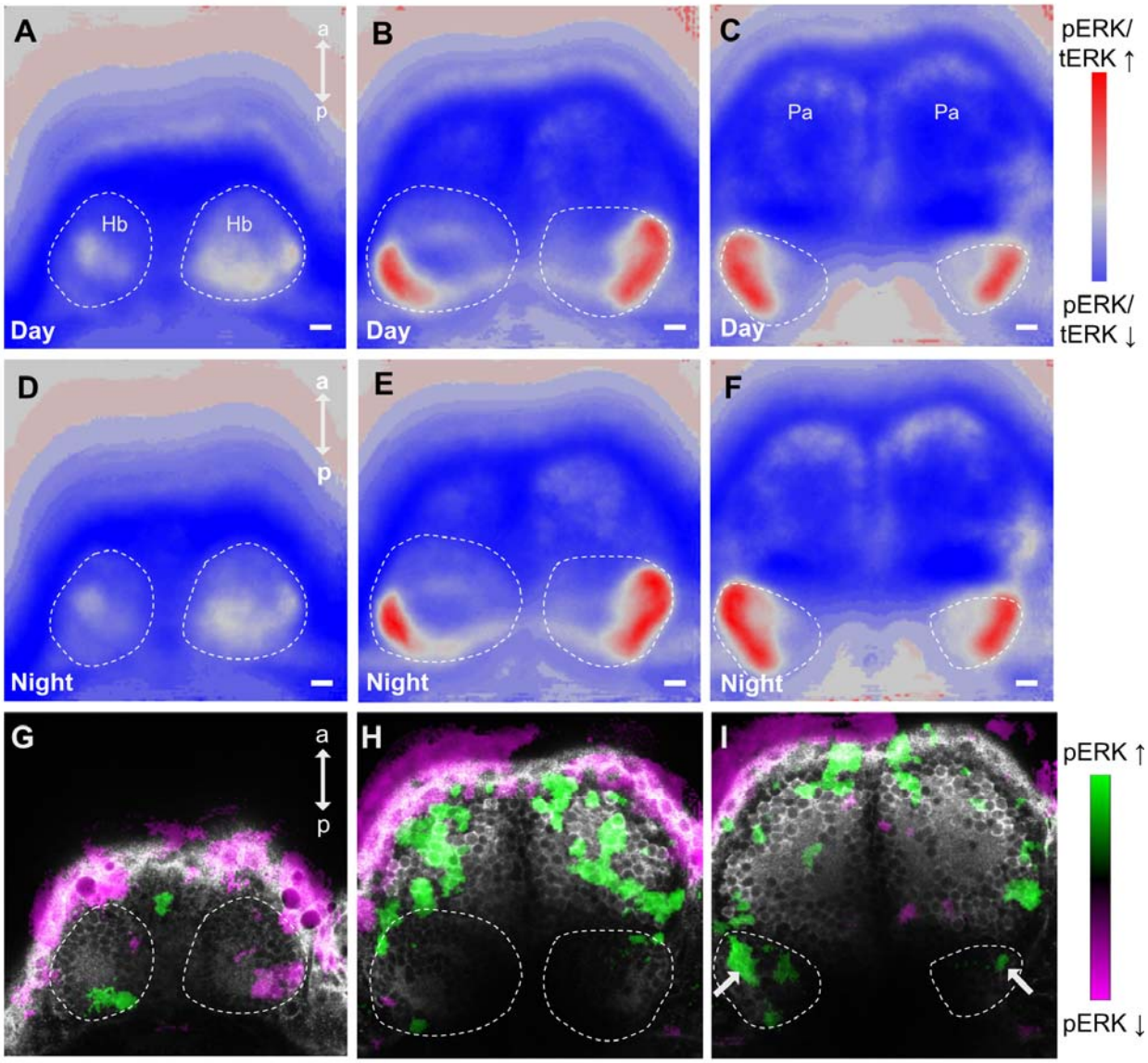

Figure 2. Habenula activity in larvae held in constant darkness. (**A-F**) Median pERK/tERK label at three different focal planes, in larvae fixed in the day (**A-C**; N = 104) or at night (**D-F**; N = 102). A and D are dorsal, B and E are intermediate, whereas C and F are deep. (**G-I**). The difference in pERK levels at Night versus Day, at the 3 different focal planes. The arrows in I indicate increased pERK in the lateral habenula. Bar = 10 µm. Contrast settings on panels A-F are identical.

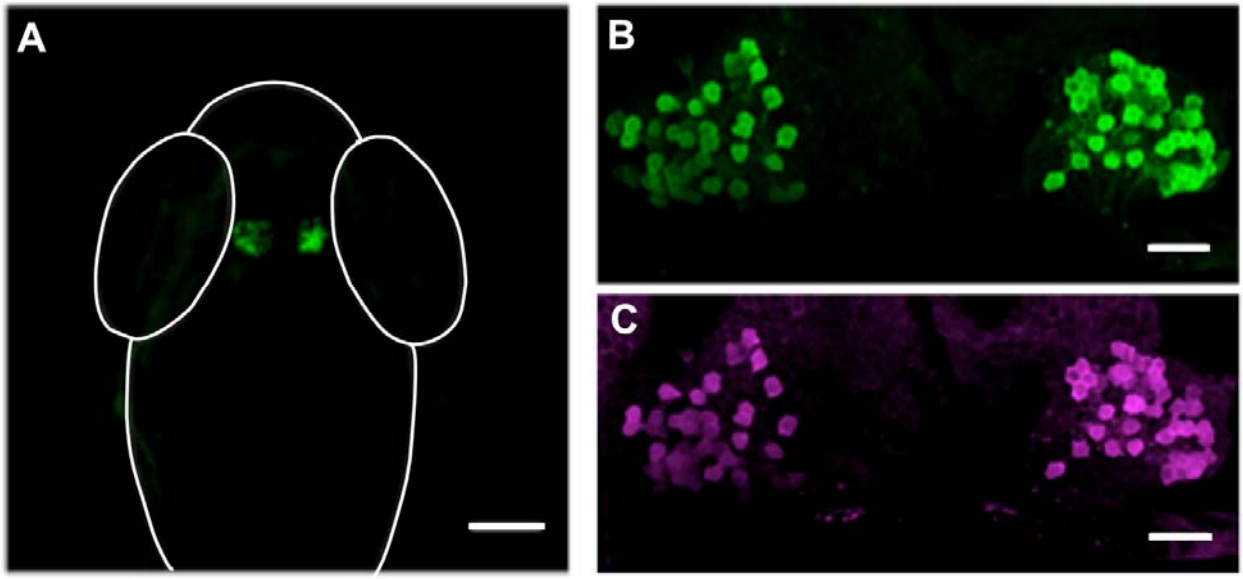

Figure 3. The *gng8:*GAL*4* driver enables expression of a C-terminus truncated *clock* gene in the habenula of zebrafish. (**A**) Specific expression of EGFP in habenula of a Tg(*gng8:GAL4, UAS:EGFP-ΔCLK*) fish. (**B**) At higher magnification, eGFP is visible in the cytoplasm of habenula neurons. (**C**) Detection of Myc, which is fused to the C-terminus of ΔCLK, in the habenula of transgenic fish. Scale bar = 100 µm in panel A, 20 µm in panels B and C.

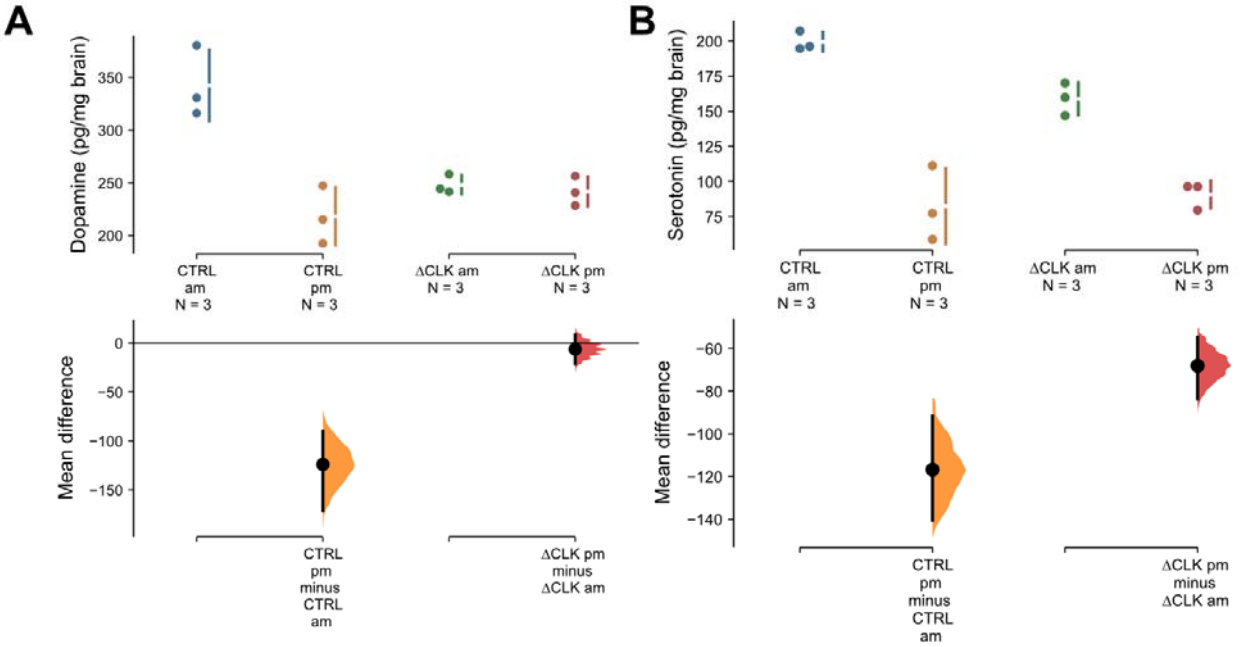

464 **Figure 4. Effects of ΔCLK expression in the habenula on global neuromodulator levels.**
465 Cumming estimation plots showing the difference in levels of dopamine (A) and serotonin (B) at
466 daytime and night-time in ΔCLK and sibling fish. The raw data is plotted on the upper axis, with
467 each dot representing a value obtained from a single brain. Gapped vertical lines to the right of each
468 group indicate mean ± SD. Mean differences are depicted on the lower axis as black dots, with the
469 vertical bars indicating bootstrap 95% CIs.
470

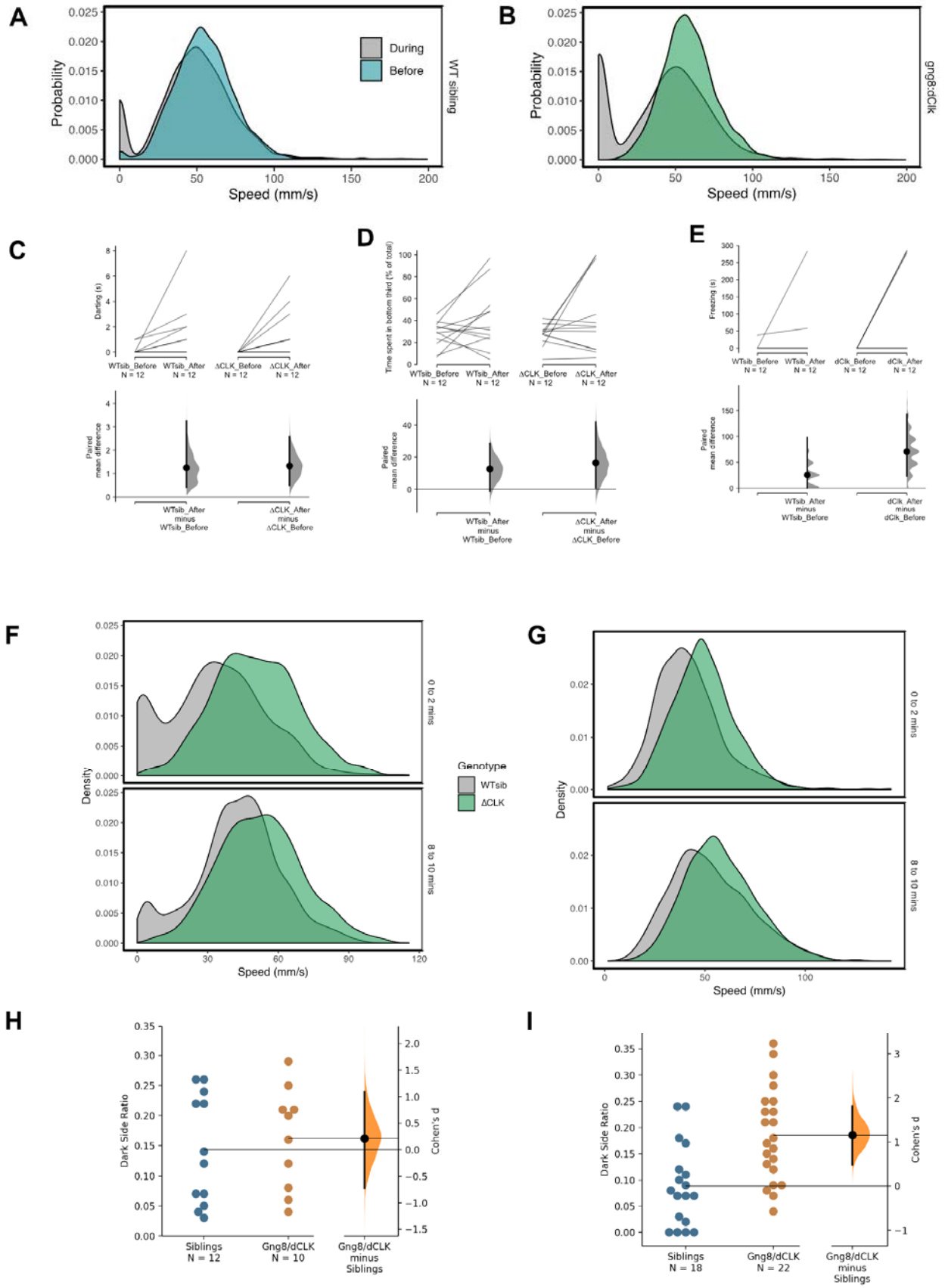
A
Probability
Speed (mm/s)
During
Before
WT sibling
B
gng8:dClk
C
Darting (s)
WTsib_Before N = 12
WTsib_After N = 12
ΔCLK_Before N = 12
ΔCLK_After N = 12
Paired mean difference
WTsib_After minus WTsib_Before
ΔCLK_After minus ΔCLK_Before
D
Time spent in bottom third (% of total)
E
Freezing (s)
dClk_Before N = 12
dClk_After N = 12
dClk_After minus dClk_Before
F
Density
0 to 2 mins
8 to 10 mins
Genotype
WTsib
ΔCLK
G
H
Dark Side Ratio
Cohen's d
Siblings N = 12
Gng8/dCLK N = 10
Gng8/dCLK minus Siblings
I
Siblings N = 18
Gng8/dCLK N = 22

471

Figure 5. The effects of *Schreckstoff* on *Tg(gng8:GAL4, UAS:EGFP-ΔCLK)* fish. (A-E) Acute effects in adult zebrafish. (**A, B**) Speed distribution in fish before and during exposure to the alarm substance Freezing, as indicated by the peak at 0 mm/s, is seen in both wildtype (A) and ΔCLK fish (B). (**C-E**) Time spent darting (C) or at the bottom third of the tank (D), or freezing (E) before and in the presence of *Schreckstoff*. There is no difference in the behaviour of fish with and without expression of truncated clocka. (**F, G**). Post-exposure behaviour in adult fish. (**F**) Histogram of speed in a novel tank containing clean water, after exposure to Schreckstoff in a separate container. Fish expressing ΔCLK in the habenula do not freeze (green shading), in contrast to their non-expressing siblings (gray shading). (**G**). Behaviour of non-exposed fish in the novel tank. No freezing was observed. (**H, I**) Post-exposure behaviour in 2 week-old zebrafish. (**H**) Percentage of time in the dark area of a tank, after 10 minutes of exposure to embryo water. (**I**) Percentage of time spent in the dark side after exposure to the alarm substance. *Tg(gng8:GAL4, UAS:EGFP-ΔCLK)* fish spend more time in the dark side, with a Cohen's D of 1.2.

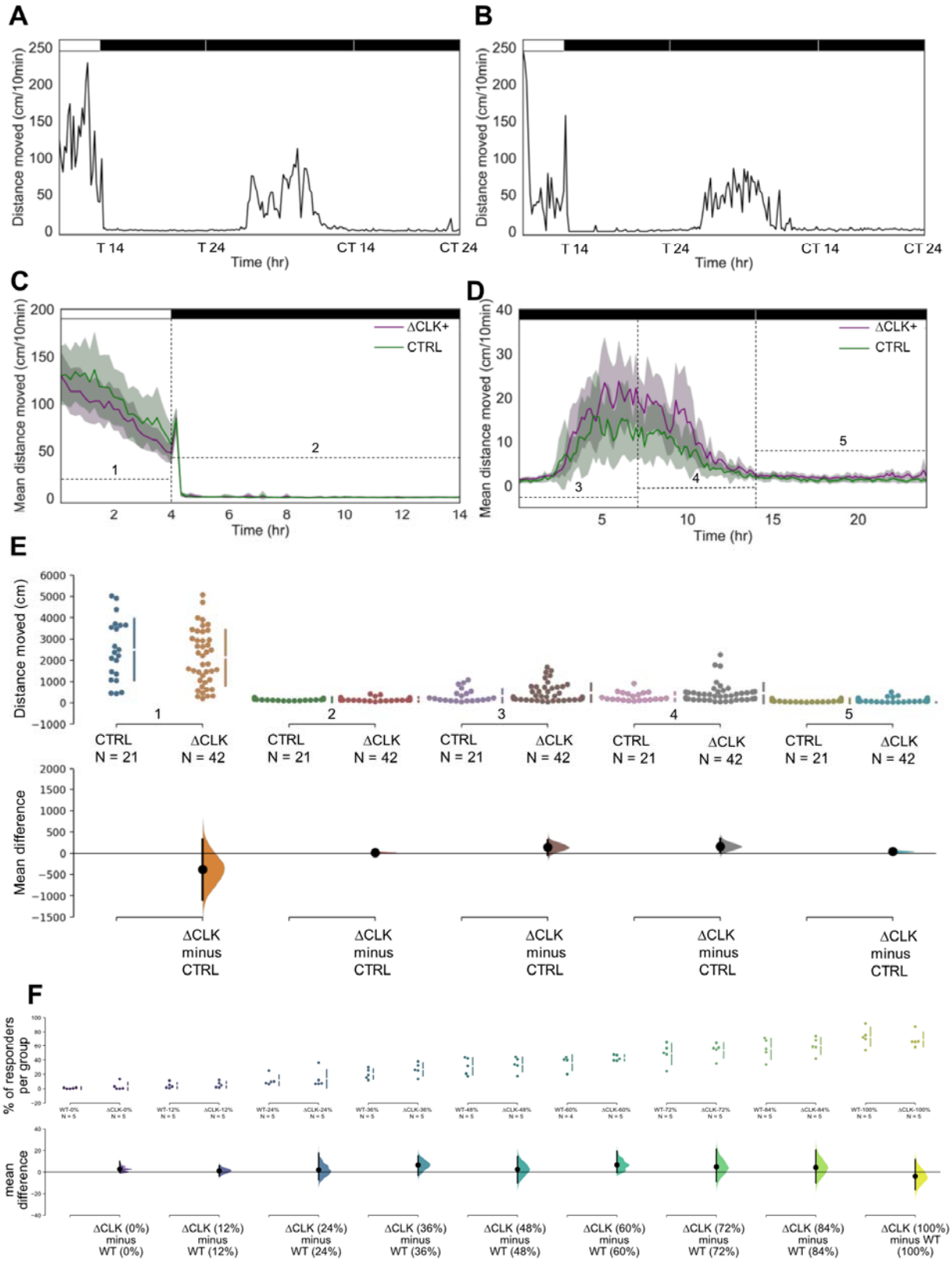
A
B
Distance moved (cm/10min)
Time (hr)
T 14
T 24
CT 14
CT 24
C
D
Mean distance moved (cm/10min)
ΔCLK+
CTRL
E
Distance moved (cm)
CTRL
N = 21
ΔCLK
N = 42
Mean difference
ΔCLK
minus
CTRL
F
% of responders
per group
mean
difference
ΔCLK (0%)
minus
WT (0%)
ΔCLK (12%)
minus
WT (12%)
ΔCLK (24%)
minus
WT (24%)
ΔCLK (36%)
minus
WT (36%)
ΔCLK (48%)
minus
WT (48%)
ΔCLK (60%)
minus
WT (60%)
ΔCLK (72%)
minus
WT (72%)
ΔCLK (84%)
minus
WT (84%)
ΔCLK (100%)
minus WT
(100%)

486

Figure 6. Circadian behaviour is unaltered in *Tg(gng8:GAL4, UAS:EGFP-ΔCLK)* larvae

(**A, B**) Distances moved (cm/10min) by individual larvae from (A) CTRL group and (B) ΔCLK+ group are plotted against time (hr) over the time-course of the whole recording. CT = circadian time. (**C, D**) Mean distances moved (cm/10min) are plotted against time (hr) (C) during the first 14 hours of recording, including 4 hours of light-phase and 10 hours in dark during the night and (D) during the subsequent 24 hours of recording under DD. CTRL (green) groups Tg(gng8:GAL4;UAS:EGFP-ΔCLK) 95% CIs are indicated by the shaded areas; interrupted lines indicate 5 analyzed timeframes. Black and white bars represent periods of dark and light, correspondingly. (**E**) The Cumming estimation plot shows the mean differences for 5 comparisons, corresponding to 5 timeframes of recording. These are 1 = light-phase; 2 = 1st night; 3 = early subjective day; 4 = late subjective day; 5 = subjective night. The raw data is plotted on the upper axis, each dot representing the overall distance moved (cm) by a single larva; gapped vertical lines to the right of each group indicate mean ± SD. Each mean difference is plotted on the lower axes as a bootstrap sampling distribution. Mean differences are depicted as black dots and 95% CIs are indicated by the end of vertical error bars. (**F**) Analysis of sensory responsiveness of the *Tg(gng8:gal4,UAS:EGFP-ΔCLK)* larvae (7 dpf) during the delivery of auditory stimuli of 9 different intensities. The Cumming estimation plot shows the mean differences for 9 comparisons, corresponding to 9 stimulus intensities (0-100%). The raw data is plotted on the upper axis, each dot representing the percentage of responders per single experimental run. (G)

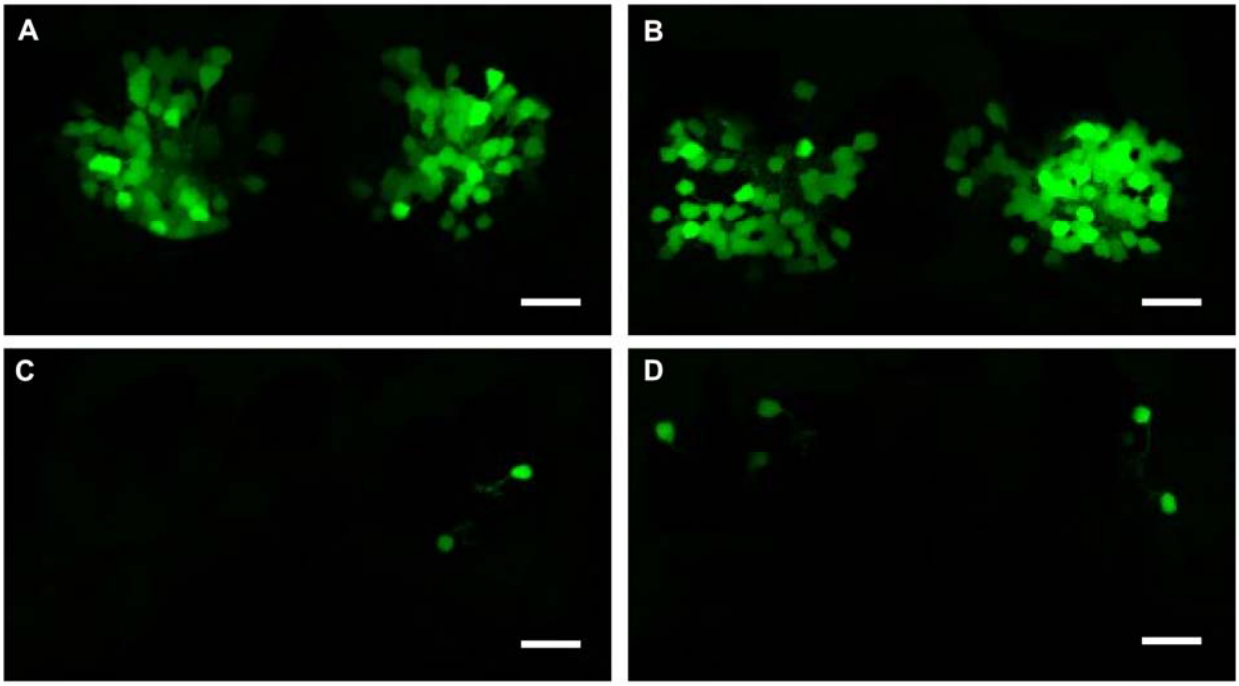

Figure S1. Examples of *Tg(gng8:GAL4, UAS:EGFP-ΔCLK)* larval zebrafish with broad (A, B) and sparse (C, D) expression of EGFP in the habenula. All images are dorsal view. Scale bar = 10 μm.

References

Abercrombie ED, Keefe KA, DiFrischia DS, Zigmond MJ. 1989. Differential effect of stress on in vivo dopamine release in striatum, nucleus accumbens, and medial frontal cortex. *J Neurochem* **52**:1655–1658.

Andalman AS, Burns VM, Lovett-Barron M, Broxton M, Poole B, Yang SJ, Grosenick L, Lerner TN, Chen R, Benster T, Mourrain P, Levoy M, Rajan K, Deisseroth K. 2019. Neuronal Dynamics Regulating Brain and Behavioral State Transitions. *Cell* **177**:970–985.e20.

Anderson DJ, Adolphs R. 2014. A framework for studying emotions across species. *Cell* **157**:187–200.

Antle MC, Silver R. 2016. Circadian Insights into Motivated Behavior. *Curr Top Behav Neurosci* **27**:137–169.

Belle MDC. 2015. Circadian Tick-Talking Across the Neuroendocrine System and Suprachiasmatic Nuclei Circuits: The Enigmatic Communication Between the

Molecular and Electrical Membrane Clocks. *J Neuroendocrinol* **27**:567–576.

Ben-Moshe Livne Z, Alon S, Vallone D, Bayleyen Y, Tovin A, Shainer I, Nisembaum LG, Aviram I, Smadja-Storz S, Fuentes M, Falcón J, Eisenberg E, Klein DC, Burgess HA, Foulkes NS, Gothilf Y. 2016. Genetically Blocking the Zebrafish Pineal Clock Affects Circadian Behavior. *PLoS Genet* **12**:e1006445.

Buijs RM. 1978. Intra- and extrahypothalamic vasopressin and oxytocin pathways in the rat. Pathways to the limbic system, medulla oblongata and spinal cord. *Cell Tissue Res* **192**:423–435.

Burgess HA, Granato M. 2007. Sensorimotor gating in larval zebrafish. *J Neurosci* **27**:4984–4994.

Cao G, Nitabach MN. 2008. Circadian control of membrane excitability in Drosophila melanogaster lateral ventral clock neurons. *J Neurosci* **28**:6493–6501.

Chaouloff F, Berton O, Mormède P. 1999. Serotonin and stress. *Neuropsychopharmacology* **21**:28S–32S.

Chastrette N, Pfaff DW, Gibbs RB. 1991. Effects of daytime and nighttime stress on Fos-like immunoreactivity in the paraventricular nucleus of the hypothalamus, the habenula, and the posterior paraventricular nucleus of the thalamus. *Brain Res* **563**:339–344.

Chatterjee D, Gerlai R. 2009. High precision liquid chromatography analysis of dopaminergic and serotoninergic responses to acute alcohol exposure in zebrafish. *Behav Brain Res* **200**:208–213.

Cheng R-K, Krishnan S, Jesuthasan S. 2016. Activation and inhibition of tph2 serotonergic neurons operate in tandem to influence larval zebrafish preference for light over darkness. *Sci Rep* **6**:20788.

Chia JSM, Wall ES, Wee CL, Rowland TAJ, Cheng R-K, Cheow K, Guillemin K, Jesuthasan S. 2019. Bacteria evoke alarm behaviour in zebrafish. *Nat Commun* **10**:3831.

Daut RA, Fonken LK. 2019. Circadian regulation of depression: A role for serotonin. *Front Neuroendocrinol* **54**:100746.

Dekens MPS, Whitmore D. 2008. Autonomous onset of the circadian clock in the zebrafish embryo. *The EMBO Journal*. doi:10.1038/emboj.2008.183

Di Rocco RT, Belanger CF, Imre I, Brown GE, Johnson NS. 2014. Daytime avoidance of chemosensory alarm cues by adult sea lamprey (Petromyzon marinus). *Can J Fish*

557 *Aquat Sci* **71**:824–830.
558 Guilding C, Hughes ATL, Piggins HD. 2010. Circadian oscillators in the epithalamus.
559 *Neuroscience* **169**:1630–1639.
560 Haghani S, Karia M, Cheng R-K, Mathuru AS. 2019. An Automated Assay System to Study
561 Novel Tank Induced Anxiety. *Front Behav Neurosci* **13**:180.
562 Ho J, Tumkaya T, Aryal S, Choi H, Claridge-Chang A. 2019. Moving beyond P values: data
563 analysis with estimation graphics. *Nat Methods* **16**:565–566.
564 Holly EN, Miczek KA. 2016. Ventral tegmental area dopamine revisited: effects of acute and
565 repeated stress. *Psychopharmacology* **233**:163–186.
566 Hong E, Santhakumar K, Akitake CA, Ahn SJ, Thisse C, Thisse B, Wyart C, Mangin J-M,
567 Halpern ME. 2013. Cholinergic left-right asymmetry in the habenulo-interpeduncular
568 pathway. *Proc Natl Acad Sci U S A* **110**:21171–21176.
569 Hughes AT, Fahey B, Cutler DJ, Coogan AN, Piggins HD. 2004. Aberrant gating of photic
570 input to the suprachiasmatic circadian pacemaker of mice lacking the VPAC2 receptor.
571 *J Neurosci* **24**:3522–3526.
572 Hume JB, Wagner M. 2018. A death in the family: Sea lamprey (Petromyzon marinus)
573 avoidance of confamilial alarm cues diminishes with phylogenetic distance. *Ecol Evol*
574 **8**:3751–3762.
575 Jesuthasan SJ, Krishnan S, Cheng R-K, Mathuru A. 2020. Larval zebrafish respond to the
576 alarm pheromone Schreckstoff by immobility and a change in brain state. *bioRxiv*.
577 doi:10.1101/2020.04.23.054734
578 Jesuthasan SJ, Mathuru AS. 2008. The alarm response in zebrafish: innate fear in a
579 vertebrate genetic model. *J Neurogenet* **22**:211–228.
580 Koch CE, Leinweber B, Drengberg BC, Blaum C, Oster H. 2017. Interaction between
581 circadian rhythms and stress. *Neurobiol Stress* **6**:57–67.
582 Li K, Zhou T, Liao L, Yang Z, Wong C, Henn F, Malinow R, Yates JR 3rd, Hu H. 2013. βCaMKII
583 in lateral habenula mediates core symptoms of depression. *Science* **341**:1016–1020.
584 Mao L-M, Wang JQ. 2016. Synaptically Localized Mitogen-Activated Protein Kinases: Local
585 Substrates and Regulation. *Mol Neurobiol* **53**:6309–6315.
586 Maximino C, Lima MG, Costa CC, Guedes IML, Herculano AM. 2014. Fluoxetine and WAY
587 100,635 dissociate increases in scototaxis and analgesia induced by conspecific alarm

substance in zebrafish (Danio rerio Hamilton 1822). *Pharmacol Biochem Behav* **124**:425–433.

McClung CA, Sidiropoulou K, Vitaterna M, Takahashi JS, White FJ, Cooper DC, Nestler EJ. 2005. Regulation of dopaminergic transmission and cocaine reward by the Clock gene. *Proc Natl Acad Sci U S A* **102**:9377–9381.

Moore HA, Whitmore D. 2014. Circadian rhythmicity and light sensitivity of the zebrafish brain. *PLoS One* **9**:e86176.

Namboodiri VMK, Rodriguez-Romaguera J, Stuber GD. 2016. The habenula. *Curr Biol* **26**:R873–R877.

Ogawa S, Nathan FM, Parhar IS. 2014. Habenular kisspeptin modulates fear in the zebrafish. *Proc Natl Acad Sci U S A* **111**:3841–3846.

Pennartz CMA, de Jeu MTG, Bos NPA, Schaap J, Geurtsen AMS. 2002. Diurnal modulation of pacemaker potentials and calcium current in the mammalian circadian clock. *Nature* **416**:286–290.

Pfeiffer W. 1962. The fright reaction of fish. *Biol Rev Camb Philos Soc* **37**:495–511.

Pfeiffer W, Riegelbauer G. 1978. The effect of the alarm substance on the central nervous excitation of the black tetraGymnocorymbus ternetzi (Characidae, Ostariophysi, Pisces) indicated by dorsal light response. *Journal of Comparative Physiology ? A*. doi:10.1007/bf00656882

Plotnikov A, Zehorai E, Procaccia S, Seger R. 2011. The MAPK cascades: signaling components, nuclear roles and mechanisms of nuclear translocation. *Biochim Biophys Acta* **1813**:1619–1633.

Prober DA, Rihel J, Onah AA, Sung R-J, Schier AF. 2006. Hypocretin/orexin overexpression induces an insomnia-like phenotype in zebrafish. *J Neurosci* **26**:13400–13410.

Randlett O, Wee CL, Naumann EA, Nnaemeka O, Schoppik D, Fitzgerald JE, Portugues R, Lacoste AMB, Riegler C, Engert F, Schier AF. 2015. Whole-brain activity mapping onto a zebrafish brain atlas. *Nature Methods*. doi:10.1038/nmeth.3581

Sakhi K, Wegner S, Belle MDC, Howarth M, Delagrange P, Brown TM, Piggins HD. 2014. Intrinsic and extrinsic cues regulate the daily profile of mouse lateral habenula neuronal activity. *J Physiol* **592**:5025–5045.

Salaberry NL, Hamm H, Felder-Schmittbuhl M-P, Mendoza J. 2019. A suprachiasmatic-

619 independent circadian clock(s) in the habenula is affected by Per gene mutations and
620 housing light conditions in mice. *Brain Struct Funct* **224**:19–31.
621 Sánchez-Bretaño A, Gueguen M-M, Cano-Nicolau J, Kah O, Alonso-Gómez ÁL, Delgado MJ,
622 Isorna E. 2015. Anatomical distribution and daily profile of gper1b gene expression in
623 brain and peripheral structures of goldfish (Carassius auratus). *Chronobiol Int* **32**:889–
624 902.
625 Scammell TE, Arrigoni E, Lipton JO. 2017. Neural Circuitry of Wakefulness and Sleep.
626 *Neuron* **93**:747–765.
627 Shearman LP, Zylka MJ, Weaver DR, Kolakowski LF Jr, Reppert SM. 1997. Two period
628 homologs: circadian expression and photic regulation in the suprachiasmatic nuclei.
629 *Neuron* **19**:1261–1269.
630 Shieh K-R. 2003. Distribution of the rhythm-related genes rPERIOD1, rPERIOD2, and
631 rCLOCK, in the rat brain. *Neuroscience* **118**:831–843.
632 Speedie N, Gerlai R. 2008. Alarm substance induced behavioral responses in zebrafish
633 (Danio rerio). *Behav Brain Res* **188**:168–177.
634 Steenbergen PJ, Richardson MK, Champagne DL. 2011. Patterns of avoidance behaviours in
635 the light/dark preference test in young juvenile zebrafish: a pharmacological study.
636 *Behav Brain Res* **222**:15–25.
637 Sun ZS, Albrecht U, Zhuchenko O, Bailey J, Eichele G, Lee CC. 1997. RIGUI, a putative
638 mammalian ortholog of the Drosophila period gene. *Cell* **90**:1003–1011.
639 Takahashi JS. 2017. Transcriptional architecture of the mammalian circadian clock. *Nat Rev*
640 *Genet* **18**:164–179.
641 Thines G, Vandenbussche E. 1966. The effects of alarm substance on the schooling
642 behaviour of Rasbora heteromorpha Duncker in day and night conditions. *Anim Behav*
643 **14**:296–302.
644 Weger M, Weger BD, Diotel N, Rastegar S, Hirota T, Kay SA, Strähle U, Dickmeis T. 2013.
645 Real-time in vivo monitoring of circadian E-box enhancer activity: a robust and
646 sensitive zebrafish reporter line for developmental, chemical and neural biology of the
647 circadian clock. *Dev Biol* **380**:259–273.
648 Woods IG, Schoppik D, Shi VJ, Zimmerman S, Coleman HA, Greenwood J, Soucy ER, Schier
649 AF. 2014. Neuropeptidergic signaling partitions arousal behaviors in zebrafish. *J*

Neurosci **34**:3142–3160.

Yang Y, Cui Y, Sang K, Dong Y, Ni Z, Ma S, Hu H. 2018. Ketamine blocks bursting in the lateral habenula to rapidly relieve depression. *Nature* **554**:317–322.

Zhao H, Rusak B. 2005. Circadian firing-rate rhythms and light responses of rat habenular nucleus neurons in vivo and in vitro. *Neuroscience* **132**:519–528.

Zhao Z, Xu H, Liu Y, Mu L, Xiao J, Zhao H. 2015. Diurnal Expression of the Per2 Gene and Protein in the Lateral Habenular Nucleus. *Int J Mol Sci* **16**:16740–16749.

Zhdanova IV, Wang SY, Leclair OU, Danilova NP. 2001. Melatonin promotes sleep-like state in zebrafish. *Brain Res* **903**:263–268.